Density Functional Theory Study on the Initial Step of the Permanganate Oxidation of Substituted Alkynes

Thomas Strassner* and Markus Busold

Anorganisch-chemisches Institut, Technische Universität München, Lichtenbergstrasse 4, D-85747 Garching bei München, Germany

Received: September 11, 2003; In Final Form: March 1, 2004

The initial step of the oxidation of alkynes by permanganate has been studied by DFT (B3LYP/6-311+G(d,p)) calculations. The influence of electron-withdrawing as well as electron-donating substituents was explored. The singlet and triplet potential energy hypersurfaces (PES) for a concerted [3 + 2] and a stepwise [2 + 2] mechanism were investigated. The crossing point between the singlet and triplet PES has been identified. The reaction proceeds via a [3 + 2] mechanism on the singlet PES with free energy activation barriers (ΔG_{298}) between 18.4 and 28.9 kcal/mol, while the lowest lying identified state is a reactive triplet intermediate. Available experimental and computed data are in good agreement. For the [2 + 2] case a reaction on the triplet surface would be preferred over the singlet, but both pathways lay well above the [3 + 2] pathway.

Introduction

Permanganate is a frequently used versatile reagent for the oxidation of unsaturated bonds, where the mechanism of the oxidation of triple bonds is much less clarified than that of double bonds. While the reaction with alkenes leads to cis-dihydroxylated products in high yields, alkynes are either cleaved with or without decarboxylation or oxidized to diketo compounds, depending on substituents[1,2] and reaction conditions.[3−5] It was also shown that hydrocarbons with triple bonds are oxidized by permanganate under water-free conditions to give diketo compounds.[3,6] The first step is experimentally known to be a two-electron process, resulting in the formation of a short-lived intermediate containing manganese(V), which then either decomposes to manganese(III) and a dioxo compound or reacts with more permanganate via complex routes. Generally it has been shown that more than one oxidation equivalent is necessary to produce high yields.[7]

The reaction of metal−oxo compounds with unsaturated bonds has been of great interest since Sharpless introduced the idea of the [2 + 2] reaction pathway (Scheme 1) for metal−oxo compounds such as OsO_4 and MnO_4^-, where the metal is directly involved in the oxidation reaction.[8] The discussion created many experiments, and with the availability of density functional theory (DFT) calculations also computational studies have been undertaken. While the mechanistic questions concerning the oxidation of alkenes by OsO_4 and MnO_4^- seem to be solved by independent density functional theory calculations,[9−14] there are no high-level DFT results available for the alkyne oxidation.

For the alkenes a clear preference was found for the [3 + 2] reaction pathway, while the mechanism of the alkyne oxidation has not been investigated computationally yet. Several experimental investigations could not identify the mechanism of the first oxidation step.[15−18] However, they could determine the rate of the reactions, and it was found that permanganate generally reacts slower with alkynes than with alkenes. Due to the multitude of intermediates and products in different spin states, not all possible pathways have been computed; we restricted the study to the initial interaction of the metal−oxo compound with the triple bond. We present density functional theory calculations on the two suggested pathways for the initial step of the oxidation reaction of alkynes by permanganate (Scheme 1) and compare them to experimentally measured activation energies.

SCHEME 1: [2 + 2] and [3 + 2] Reaction Pathways for the Initial Step of Permanganate Oxidation of Alkynes

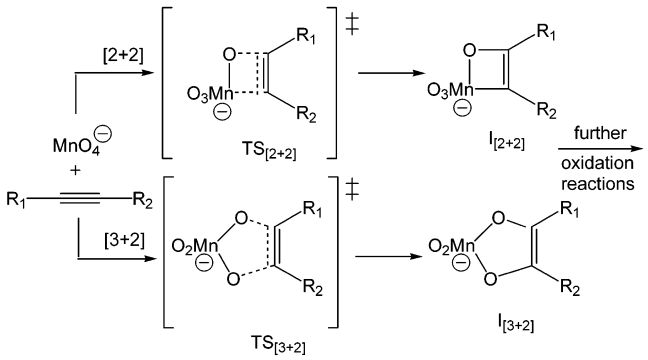

Lee et al. experimentally studied the oxidation of 1-phenyl-1-butyne and the corresponding α-keto alkyne. They observed a significant increase of the reaction rate for the α-keto alkyne and proposed that the reaction follows a [2 + 2] reaction pathway, requiring several rearrangements to explain the products.[15]

This was in contrast to earlier publications of Simandi et al.,[16−18] who had published kinetic studies on several substituted alkynes proposing that the oxidation follows a [3 + 2] pathway. We compare ethyne (**1**), 2-butyne (**2**), its α-keto derivative 2-pentyn-4-one (**3**), and but-2-yne-1,4-diol (**4**), which was experimentally found to show an activation enthalpy (ΔH_{298}) of 5.26 kcal/mol.[16−18]

* Corresponding author. Current address: Institut für Organische Chemie, Technische Universität Dresden, Mommsenstr. 13, D-01062, Dresden, Germany. Fax: ++49 (0) 351/4633-9679. E-mail: thomas.strassner@chemie.tu-dresden.de.

10.1021/jp0310652 CCC: $27.50
Published on Web 04/27/2004

SCHEME 2: Singlet and Triplet Surfaces for the Oxidation of Ethyne 1 via the [3 + 2] and [2 + 2] Pathway[a]

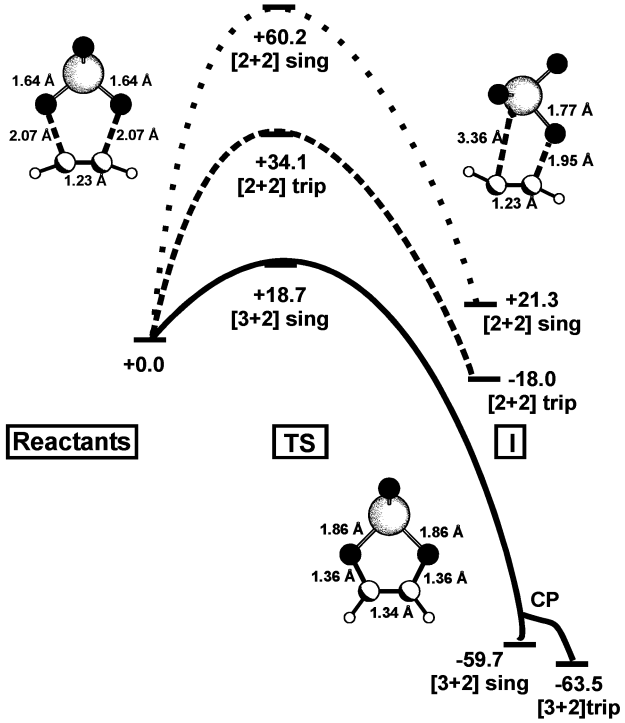

[a] Free energies (ΔG_{298}) are given in kcal/mol.

TABLE 1: Comparison of Calculated Free Energies (B3LYP/6-311+G(d,p), ΔG_{298}), Enthalpies (B3LYP/6-311+G(d,p), ΔH_{298}), and Experimental Values for Transition States (TS) and Intermediates (I) in Permanganate Alkyne Oxidation on Singlet (s) and Triplet (t) Surfaces

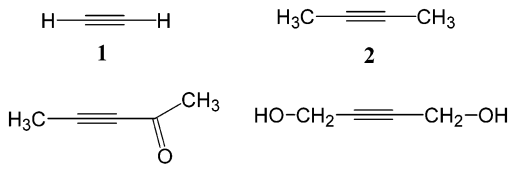

	1	2	3	4
expt			faster than 2	5.26
$\Delta H_{TS\,3+2}$	12.3 (s)	15.6 (s)	5.5 (s)	5.6 (s)
$\Delta G_{TS\,3+2}$	18.7 (s)	28.9 (s)	18.9 (s)	18.4 (s)
$\Delta H_{TS\,2+2}$	55.5 (s)	58.1 (s)	50.4 (s)	44.8 (s)
	31.1 (t)	29.7 (t)	25.4 (t)	19.3 (t)
$\Delta G_{TS\,2+2}$	60.2 (s)	69.7 (s)	62.3 (s)	42.8 (s)
	34.1 (t)	40.8 (t)	35.3 (t)	30.3 (t)
$\Delta H_{I\,3+2}$	−66.8 (s)	−63.5 (s)	−79.9 (s)	−79.1 (s)
	−68.6 (t)	−64.3 (t)	−75.1 (t)	−80.0 (t)
$\Delta G_{I\,3+2}$	−59.7 (s)	−49.1 (s)	−65.2 (s)	−64.5 (s)
	−63.5 (t)	−50.8 (t)	−63.2 (t)	−67.1 (t)
$\Delta H_{I\,2+2}$	15.0 (s)	17.7 (s)	8.1 (s)	3.0 (s)
	−21.2 (t)	nc (t)	nc (t)	nc (t)
$\Delta G_{I\,2+2}$	21.3 (s)	31.0 (s)	21.6 (s)	3.7 (s)
	−18.0 (t)	nc (t)	nc (t)	nc (t)

[a] All energies are given in kcal/mol. nc, not computed.

Computational Details

The density functional/Hartree−Fock hybrid model Becke-3LYP[19−22] as implemented in Gaussian 98[23] has been used throughout this study together with the valence triple-ζ basis set 6-311+G(d,p).[24−27] All geometries have been fully optimized; no symmetry or internal coordinate constraints were applied during optimizations. All reported intermediates were verified as true minima by the absence of negative eigenvalues in the vibrational frequency analysis. Transition-state structures (indicated by TS) were located using the Berny algorithm[28] until the Hessian matrix had only one imaginary eigenvalue. The identity of all transition states was confirmed by animating the negative eigenvector coordinate with MOLDEN.[29]

Internal reaction coordinate calculations connecting transition states with products and educts were performed, and the stability of the wave function was checked.

Approximate free energies and enthalpies were obtained through thermochemical analysis of the frequency calculation, using the thermal correction to Gibbs free energy as reported by Gaussian 98. This takes into account zero-point effects, thermal enthalpy corrections, and entropy. All energies reported in this paper, unless otherwise noted, are free energies at 298 K, using unscaled frequencies.

The MECP program of J. N. Harvey was used to locate spin crossing points between the singlet and triplet surfaces.[30]

Results and Discussion

Oxidation processes of metal−oxo compounds always involve different oxidation states and may therefore proceed on different hypersurfaces. It is also known that radical intermediates contribute to the observed bond breaking. The picture shown in Scheme 2 for the oxidation of ethyne **1** can be seen as a general scheme for all compounds investigated here. The transition states with the lowest activation enthalpy are in all cases the [3 + 2] transition states on the singlet surface.

Substituents at the triple bond, depending on whether they are donating or withdrawing electron density, change the height of the free energy barriers for **1**−**4** (18.4−28.9 kcal/mol, Table 1). The reaction of **1** is exothermic (−66.8 kcal/mol) with an activation enthalpy of +12.3 kcal/mol for the [3 + 2] transition state as well as exergonic (−59.7 kcal/mol); the corresponding free activation energy for the [3 + 2] transition state is calculated as +18.7 kcal/mol. Almost at the product stage a change from the singlet to the triplet hypersurface happens, leading to the [3 + 2] intermediate on the triplet surface. The energy differences between the [3 + 2] intermediates of differing spin are small (ΔH_{298}, 1.8 kcal/mol; ΔG_{298}, 3.8 kcal/mol), and the molecular geometries are very similar. The large negative activation entropy indicates that the structure of the transition state is highly ordered as is the case for a cyclic structure and reflects the associative nature of the reaction. The calculated barriers also explain why alkynes react slower with permanganate compared to alkenes, where the activation energies are calculated to be around 10 kcal/mol, depending on the substituents. On the triplet surface no [3 + 2] transition states could be found. The crossing point is located very close above the singlet and triplet intermediates (marked as CP in Scheme 2).

In the [2 + 2] case the enthalpies of activation for the singlet (+55.5 kcal/mol) and triplet (+31.1 kcal/mol) transition states are considerably higher as are the free energies of activation (60.2 and 34.1 kcal/mol, respectively; Table 1). These lead to singlet (ΔH_{298}, +15.0 kcal/mol; ΔG_{298}, +21.3 kcal/mol) and triplet (ΔH_{298}, −21.2 kcal/mol; ΔG_{298}, −18.0 kcal kcal/mol) intermediates which are more unfavorable than the corresponding intermediates for the [3 + 2] pathway, but obviously want to stay on the triplet surface, which is in good agreement with the calculated structure for the [2 + 2] transition state, where the bond between the oxygen and one carbon is formed while

the manganese−carbon distance is 3.36 Å, creating spin density on the other carbon and the manganese atom.

More donating substituents, such as methyl groups in the case of **2**, increase the free energy activation barriers for transition states on the singlet surface significantly by about 10 kcal/mol. Compounds **3** (the α-keto derivative of **2**) and **4** show that electron-withdrawing groups have almost no effect on the free energy barrier. However, in looking at the free enthalpy values a significant difference shows up. In agreement with experimental results reported by Lee, who found a significant increase of the reaction rate for an α-keto compound, the free enthalpy is significantly lowered by 10.1 kcal/mol comparing **3** and **2**.

The calculated free activation enthalpies of **3** (+5.5 kcal/mol) and **4** (+5.6 kcal/mol) are significantly lower in energy and in very good agreement with the experimentally observed value of 5.3 kcal/mol for **4**, although the study does not account for solvent effects which might change the barriers.

The [2 + 2] transition states for all substituted compounds, regardless of the spin, are well above the [3 + 2] pathway with the triplet [2 + 2] transition states always lower in energy (ΔH_{298}, 25.4−31.1 kcal/mol; ΔG_{298}, 34.1−40.8 kcal/mol) compared to those on the singlet surface (ΔH_{298}, 44.8−58.1 kcal/mol; ΔG_{298}, 42.8−69.7 kcal/mol).

Due to the asymmetry of compound **3**, two different [2 + 2] transition states are possible. Despite an extensive search only the [2 + 2] transition state for R_1=CO−CH_3 and R_2=CH_3 (Scheme 1) could be found. The influence of the carbonyl group can be seen in the asymmetric [3 + 2] transition state geometry of **3** compared to the symmetrical [3 + 2] transition state for **1** with C−O bond lengths of 2.07 Å each and a C−C bond length of 1.23 Å (shown in Figure 1, left side). The same asymmetry can also be found for compounds such as propargyl chloride and bromide, whose [3 + 2] transition states are very similar compared to **3**. The effect of the electron donation also shows up in the difference of 0.03 Å for the forming C−O bonds of the transition states for **1** and **2** (Figure 1). The asymmetrical transition state of compound **4** with C−O bond lengths of 2.07 and 2.13 Å results from the interaction of the two CH_2–OH groups. We also calculated the transition state where both hydroxyl groups are not interacting with each other, which is 2 kcal/mol higher in energy. For **3** the weak interaction between the α-carbon and the oxygen with a distance of 2.35 Å results in a shorter Mn−O bond with 1.62 Å. This resembles an almost educt-like (1.59 Å) double bond, while at the *β*-carbon this results in a short C−O bond (1.93 Å) and a longer Mn−O bond (1.65 Å) compared to all other transition state structures computed.

The corresponding [3 + 2] triplet intermediates for **1** and **2** (Figure 1, right side) are symmetrical and show typical bond lengths for a C−C double bond with 1.36 and 1.37 Å. All other bond lengths are very similar, and the influence of the methyl substituent on the geometry of the intermediate is small. The [3 + 2] intermediate of compound **4** (singlet surface) is also symmetrical and very similar to **1** in all the monitored bond lengths which are in some cases only 0.01 Å longer.

A quite large asymmetry is true for the corresponding minima of **3**. The asymmetric C−O bond lengths of **3** with 1.33 and 1.38 Å are significantly different from the [3 + 2] triplet intermediate of **1** with symmetrical C−O bond lengths of 1.36 Å (Scheme 2, center bottom). The asymmetry of the bond lengths carries through to Mn−O bond lengths which also differ by 0.04 Å.

In this case the formed double bond is extended to a length of 1.37 Å, an unusually long double bond due to the delocalization effect of the α-oxo group. This is confirmed by the adjacent bond which is considerably shorter compared to a normal single bond with a length of 1.45 Å. Except for **3** the former C−C triple bond length and the Mn−O bond lengths are in all cases equal or have a maximal deviation of ±0.02 Å.

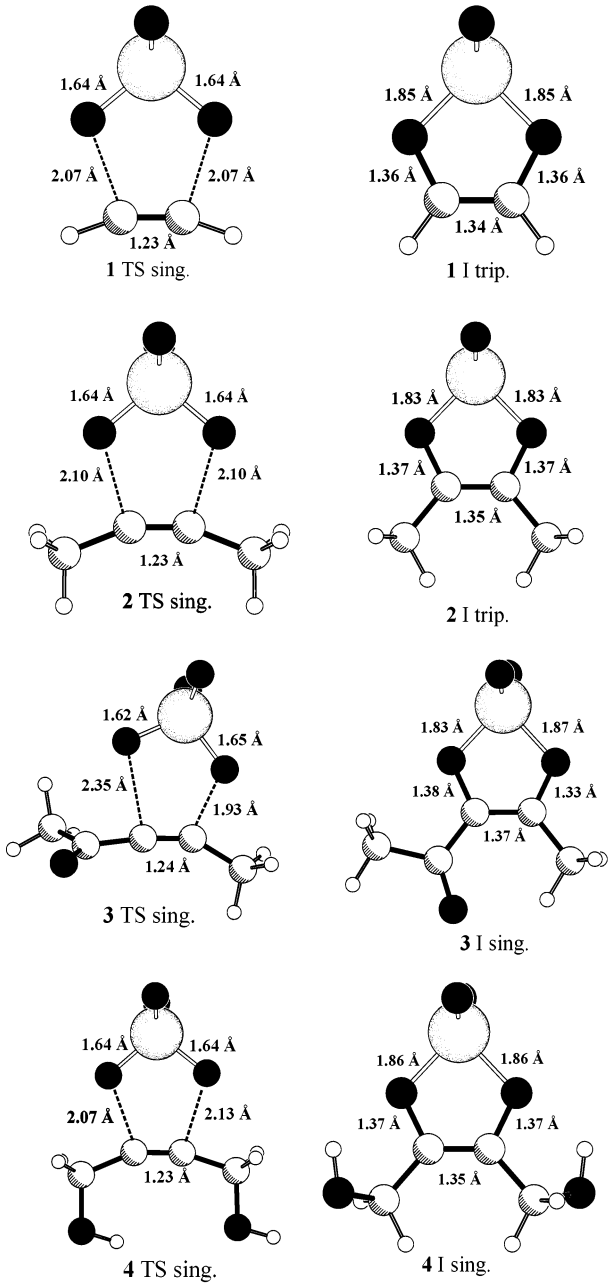

Figure 1. Geometries and selected bond lengths of the [3 + 2] transition states and intermediates with the lowest energies for all compounds. All bond lengths listed in angstroms.

The earliest transition state on the reaction coordinate is calculated for **2** with bond lengths of 2.10 Å for the C−O bond length in the [3 + 2] transition state, in agreement with the highest activation enthalpy calculated.

The geometries of the [2 + 2] transition states on the triplet surface are in general very similar (Table 2), but can no longer be called concerted. The interaction between the carbon and the oxygen atom occurs while the manganese does not closely interact with the alkyne substrate. The C−C bond length is in all cases 1.23 or 1.24 Å, which is also true for the [3 + 2] transition states. The C−O bond lengths are calculated to be 1.97 ± 0.02 Å. The most notable difference among those four

TABLE 2: Comparison of Selected [2 + 2] Transition State Bond Lengths on the Triplet Surface (in Å)

	Mn−O	C−O	C−C	Mn−C
1	1.77	1.95	1.23	3.36
2	1.77	1.98	1.23	3.40
3	1.77	1.99	1.24	3.26
4	1.77	1.97	1.23	3.28

compounds occurs in the Mn−C bond length, which is shorter for the compounds with electron-withdrawing groups **3** (3.26 Å) and **4** (3.28 Å). **2**, with the electron-donating methyl groups, shows the largest distance with 3.40 Å.

Conclusion

We can conclude that the initial steps of the alkyne oxidation by permanganate proceed via a [3 + 2] transition state on the singlet surface. This leads to intermediates which change the hypersurface close to the product state. The experimentally observed increase in the reaction rate for the oxidation of α-keto alkynes is kinetically favored over alkynes with donating substituents.

Acknowledgment. We are indebted to Prof. W. A. Herrmann for his generous and continuous support of our work and to Prof. H. Zipse for helpful discussions. We are grateful to the Leibniz-Rechenzentrum München for providing the necessary computer time.

References and Notes

(1) Fatiadi, A. J. *Synthesis* **1987**, 85−127.
(2) Walsh, C. J.; Mandal, B. K. *J. Org. Chem.* **1999**, *64*, 6102−6105.
(3) Lee, D. G.; Chang, V. S. *Synthesis* **1978**, 462−463.
(4) Srinivasan, N. S.; Lee, D. G. *J. Org. Chem.* **1979**, *44*, 1574.
(5) Lai, S.; Lee, D. G. *Tetrahedron* **2002**, *58*, 9879−9887.
(6) Lee, D. G.; Chang, V. S. *J. Org. Chem.* **1979**, *44*, 2726−2730.
(7) Tatlock, J. H. *J. Org. Chem.* **1995**, *60*, 6221−6223.
(8) Sharpless, K. B.; Teranishi, A. Y.; Backvall, J. E. *J. Am. Chem. Soc.* **1977**, *99*, 3120−3128.
(9) Pidun, U.; Boehme, C.; Frenking, G. *Angew. Chem., Int. Ed. Engl.* **1997**, *35*, 2817−2820.
(10) Dapprich, S.; Ujaque, G.; Maseras, F.; Lledos, A.; Musaev, D. G.; Morokuma, K. *J. Am. Chem. Soc.* **1996**, *118*, 11660−11661.
(11) Torrent, M.; Deng, L.; Duran, M.; Sola, M.; Ziegler, T. *Organometallics* **1997**, *16*, 13−19.
(12) DelMonte, A. J.; Haller, J.; Houk, K. N.; Sharpless, K. B.; Singleton, D. A.; Strassner, T.; Thomas, A. A. *J. Am. Chem. Soc.* **1997**, *119*, 9907−9908.
(13) Houk, K. N.; Strassner, T. *J. Org. Chem.* **1999**, *64*, 800−802.
(14) Strassner, T.; Busold, M. *J. Org. Chem.* **2001**, *66*, 672−676.
(15) Lee, D. G.; Lee, E. J.; Chandler, W. D. *J. Org. Chem.* **1985**, *50*, 4306−4309.
(16) Simandi, L.; Miklos, J. *Magy. Kem. Foly.* **1978**, *84*, 512−518.
(17) Simandi, L. I.; Jaky, M. *J. Chem. Soc., Perkin Trans. 2* **1973**, 1861−1866.
(18) Simandi, L. I.; Jaky, M. *J. Chem. Soc., Perkin Trans. 2* **1977**, 630−633.
(19) Lee, C.; Yang, W.; Parr, R. G. *Phys. Rev. B: Condens. Matter* **1988**, *37*, 785−789.
(20) Stephens, P. J.; Devlin, F. J.; Chabalowski, C. F.; Frisch, M. J. *J. Phys. Chem.* **1994**, *98*, 11623−11627.
(21) Vosko, S. H.; Wilk, L.; Nusair, M. *Can. J. Phys.* **1980**, *58*, 1200−1211.
(22) Becke, A. D. *J. Chem. Phys.* **1993**, *98*, 5648−5652.
(23) Frisch, M. J.; Trucks, G. W.; Schlegel, H. B.; Scuseria, G. E.; Robb, M. A.; Cheeseman, J. R.; Zakrzewski, V. G.; Montgomery, J. A., Jr.; Stratmann, R. E.; Burant, J. C.; Dapprich, S.; Millam, J. M.; Daniels, A. D.; Kudin, K. N.; Strain, M. C.; Farkas, O.; Tomasi, J.; Barone, V.; Cossi, M.; Cammi, R.; Mennucci, B.; Pomelli, C.; Adamo, C.; Clifford, S.; Ochterski, J.; Petersson, G. A.; Ayala, P. Y.; Cui, Q.; Morokuma, K.; Malick, D. K.; Rabuck, A. D.; Raghavachari, K.; Foresman, J. B.; Cioslowski, J.; Ortiz, J. V.; Stefanov, B. B.; Liu, G.; Liashenko, A.; Piskorz, P.; Komaromi, I.; Gomperts, R.; Martin, R. L.; Fox, D. J.; Keith, T.; Al-Laham, M. A.; Peng, C. Y.; Nanayakkara, A.; Gonzalez, C.; Challacombe, M.; Gill, P. M. W.; Johnson, B.; Chen, W.; Wong, M. W.; Andres, J. L.; Gonzalez, C.; Head-Gordon, M.; Replogle, E. S.; Pople, J. A. *Gaussian 98*, revision A7; Gaussian, Inc.: Pittsburgh, 1998.
(24) Krishnan, R.; Binkley, J. S.; Seeger, R.; Pople, J. A. *J. Chem. Phys.* **1980**, *72*, 650−654.
(25) Hay, P. J. *J. Chem. Phys.* **1977**, *66*, 4377−4384.
(26) Wachters, A. J. H. *J. Chem. Phys.* **1970**, *52*, 1033−1036.
(27) Raghavachari, K.; Trucks, G. W. *J. Chem. Phys.* **1989**, *91*, 1062−1065.
(28) Schlegel, H. B. *J. Comput. Chem.* **1982**, *3*, 214.
(29) Noordik, G. S. J. H. *J. Comput.-Aided Mol. Des.* **2000**, *14*, 123−134.
(30) Harvey, J. N.; Aschi, M.; Schwarz, H.; Koch, W. *Theor. Chem. Acc.* **1998**, *99*, 95−99.